Supporting Information

A Non-Isolated Pentagon Rule C_{82} Cage Stabilized by a Stretched Sc_3N Cluster

Min Guo,[a†] Xiaomeng Li,[a†] Yang-Rong Yao,[b] Jiaxin Zhuang,[a] Qingyu Meng,[a] Yingjing Yan,[a] Xinye Liu[a] and Ning Chen[a*]

[a] *College of Chemistry, Chemical Engineering and Materials Science, and State Key Laboratory of Radiation Medicine and Protection, Soochow University, Suzhou, Jiangsu 215123, P.R. China. Email: chenning@suda.edu.cn*

[b] *Department of chemistry, University of Texas at El Paso. 500W University Avenue, El Paso, Texas 79968, USA*

†These authors contribute equally to this work.

Table of Contents

Experimental Details

Synthesis of $Sc_3N@C_s(39663)$-C_{82}. $Sc_3N@C_s(39663)$-C_{82} was synthesized by a modified Krätschmer-Huffman DC arc-discharge method. Each graphite rod packed with a mixture of Sc_2O_3 and graphite powder (molar ratio of Sc/C = 1:24) was vaporized in the arcing chamber under 266 mbar He and 5 mbar N_2 atmosphere. The resulting raw soot was collected and extracted with CS_2 for 12 h. On the average ca. 30 mg of crude fullerene mixture per rod was obtained. Finally, 150 graphite rods was vaporized and ca. 0.8 mg $Sc_3N@C_s(39663)$-C_{82} was obtained. Besides $Sc_3N@C_s(39663)$-C_{82}, ca. 0.2 mg $Sc_3N@C_{2v}(39718)$-C_{82} was obtained and other scandium-based endohedral fullerenes $Sc@C_{2n}$ and $Sc_3N@C_{2n}$ were also formed along with empty fullerenes during arcing progress.

High performance liquid chromatography (HPLC) separation process of $Sc_3N@C_s(39663)$-C_{82}. The first stage was performed on a Buckyprep-M column (25 mm × 250 mm, Cosmosil Nacalai Tesque) with toluene as mobile phase. After that, as shown in Figure S1, fraction 9 (from 34 to 60 min, marked in orange) was re-injected into a Buckyprep column (10mm × 250 mm, Cosmosil Nacalai Tesque) for the second stage separation using toluene as the eluent. The fraction marked in green which contained $Sc_3N@C_s(39663)$-C_{82} was collected. The third stage of separation was conducted on a 5PBB column (10mm × 250 mm, Cosmosil Nacalai Tesque) with toluene as the eluent. The fraction marked in cyan which contained $Sc_3N@C_s(39663)$-C_{82} was collected. The last stage separation was conducted on a Buckyprep-M column (10mm × 250 mm, Cosmosil Nacalai Tesque) using toluene as the eluent and pure $Sc_3N@C_s(39663)$-C_{82} was got. The purity of the isolated $Sc_3N@C_s(39663)$-C_{82} was reconfirmed by chromatography on a Buckyprep-M column with toluene at the flow rate 4 mL/min, along with MALDI-TOF mass spectrometry in a positive charge mode. The wavelength of detection used for HPLC was 310 nm.

High performance liquid chromatography (HPLC) separation process of $Sc_3N@C_{2v}(39718)$-C_{82}. The first stage was performed on a Buckyprep-M column (25 mm × 250 mm, Cosmosil Nacalai Tesque) with toluene as mobile phase. After that, as shown in Figure S2, fraction 8 (from 28 to 33 min, marked in red) was re-injected into a Buckyprep column (10mm × 250 mm, Cosmosil Nacalai Tesque) for the second stage separation using toluene as the eluent. The fraction marked in yellow which contained $Sc_3N@C_{2v}(39718)$-C_{82} was collected. The third stage of separation was conducted on a 5PBB column (10mm × 250 mm, Cosmosil Nacalai Tesque) with toluene as the eluent. The

fraction marked in orange which contained $Sc_3N@C_{2v}(39718)$-C_{82} was collected. The last stage separation was recycled on a 5PBB column (10mm × 250 mm, Cosmosil Nacalai Tesque) using toluene as the eluent and pure $Sc_3N@C_{2v}(39718)$-C_{82} was got. The purity of the isolated $Sc_3N@C_{2v}(39718)$-C_{82} was reconfirmed by chromatography on a Buckyprep-M column with toluene at the flow rate 4 mL/min, along with MALDI-TOF mass spectrometry in a positive charge mode. The wavelength of detection used for HPLC was 310 nm.

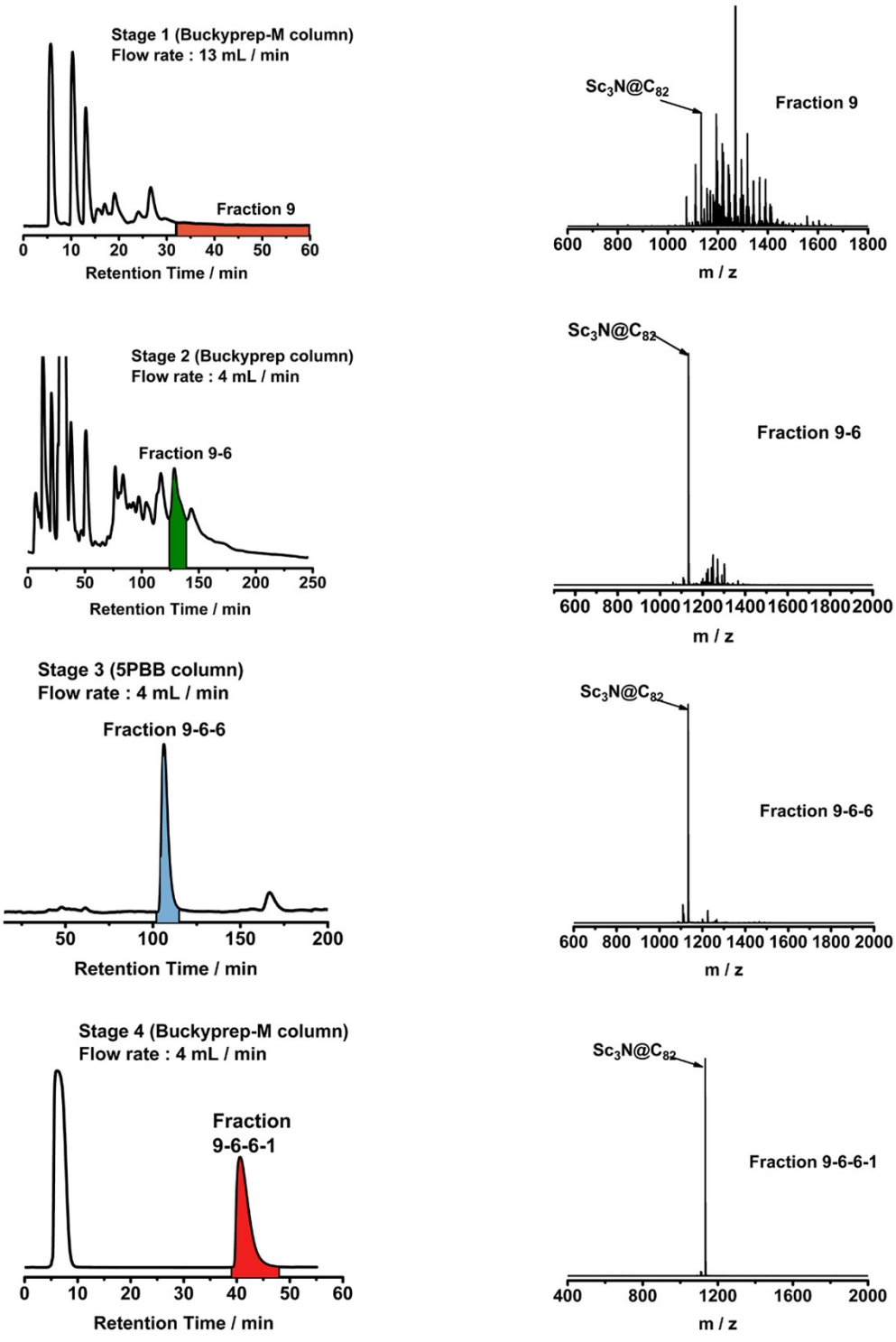

Fig. S1 HPLC profiles showing the separation of $Sc_3N@C_s(39663)$-C_{82} (left) and the corresponding MALDI-TOF mass spectra (right).

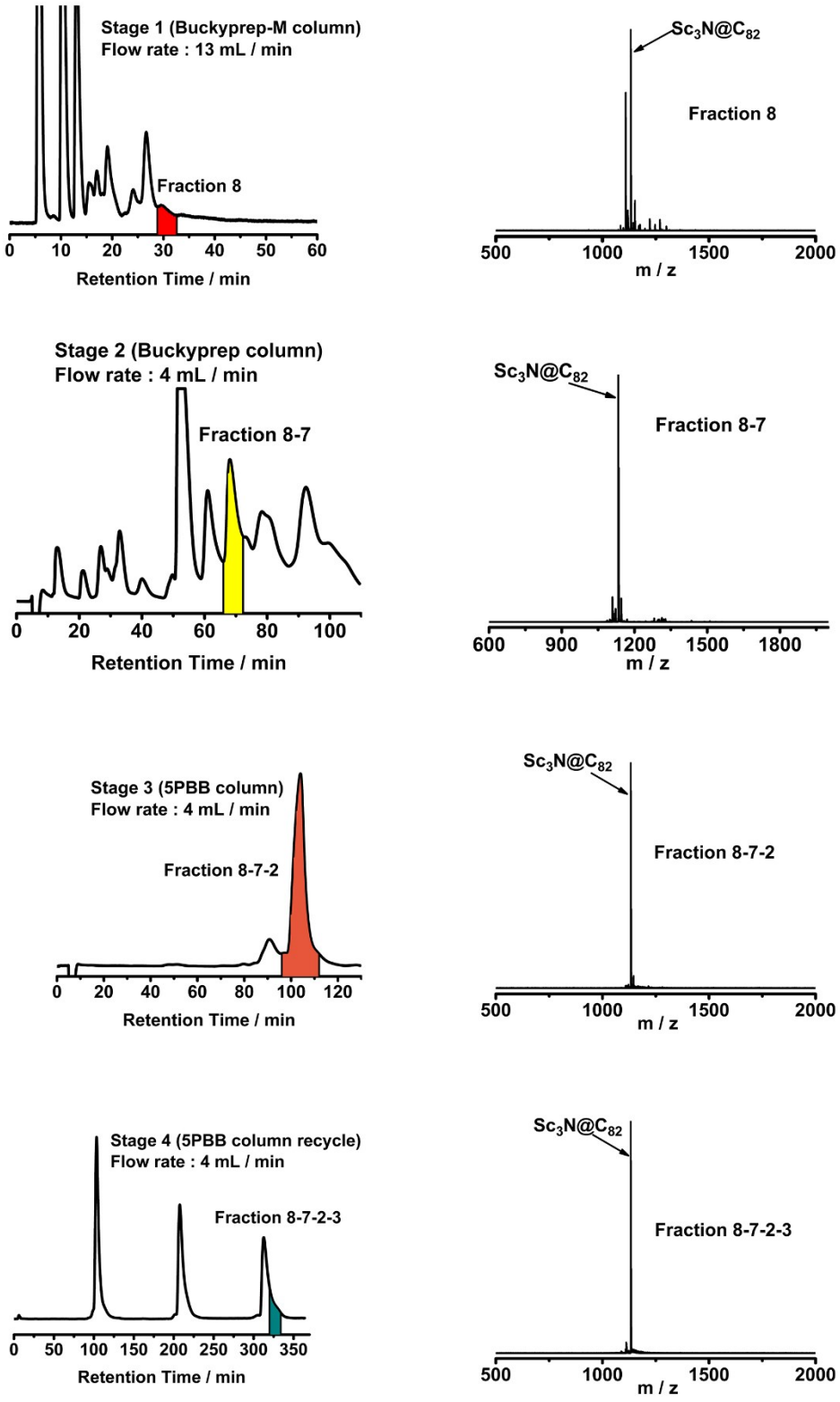

Fig. S2 HPLC profiles showing the separation of $Sc_3N@C_{2v}(39718)$-C_{82} (left) and the corresponding MALDI-TOF mass spectra (right).

Electrochemical studies of $Sc_3N@C_s$(39663)-C_{82}. Cyclic voltammetry (CV) was obtained in *o*-dichlorobenzene using a CHI-660E instrument. A conventional three-electrode cell consisting of a platinum counter-electrode, a glassy carbon working electrode, and a silver reference electrode was used for the measurement. $(n\text{-}Bu)_4NPF_6$ (0.05 M) was used as the supporting electrolyte. The CV was measured at a scan rate of 100 mV/s.

Spectroscopic studies of $Sc_3N@C_s$(39663)-C_{82} and $Sc_3N@C_{2v}$(39718)-C_{82}. The positive-ion mode matrix assisted laser desorption/ionization time-of-flight (Bruker, German) was employed for the mass characterization. UV−vis−NIR spectrum of the purified $Sc_3N@C_s$(39663)-C_{82} and $Sc_3N@C_{2v}$(39718)-C_{82} was measured in CS_2 solution with a Cary 5000 UV−vis−NIR spectrophotometer (Agilent, USA).

Single-Crystal X-ray Diffraction. Black cocrystals of $Sc_3N@C_s$(39663)-C_{82}·[Ni^{II}(OEP)] ·C_6H_6 were obtained by allowing a solution of the fullerene in CS_2 and a solution of [Ni^{II}(OEP)] in benzene to diffuse together. X-ray data were collected at 130 K using a diffractometer (APEX II; Bruker Analytik GmbH) equipped with a CCD collector. The multi-scan method was used for absorption correction. The structure was resolved using direct methods[1] (SIR2004) and refined on F^2 using full-matrix least-squares using SHELXL2015.[2] Hydrogen atoms were inserted at calculated positions and constrained with isotropic thermal parameters.

Crystal data for $Sc_3N@C_s$(39663)-C_{82}·[Ni^{II}(OEP)] ·C_6H_6: C124 H50 N5 Ni Sc3, M_r = 1803.28, 0.2 × 0.15 × 0.08 mm^3 , monoclinic, space group $P2_1/c$ (No. 14), a = 19.830(5) Å, b = 15.111(3) Å, c = 25.233(8) Å, α = 90°, β = 93.958(19)°, γ = 90°, V = 7543(3) $Å^3$, Z = 4, ρ_{calcd} = 1.588 g cm^{-3}, μ(Cu Kα) = 3.039mm^{-1}, ϑ = 2.233− 68.331°, T = 130(2) K, R_1 = 0.0921, wR_2 = 0.2368 for all data; R_1 = 0.0794, wR_2 = 0.2210 for 11277 reflections ($I > 2.0\sigma(I)$) with 1233 parameters. Goodness of fit indicator 1.057. Maximum residual electron density 1.353 e $Å^{-3}$.

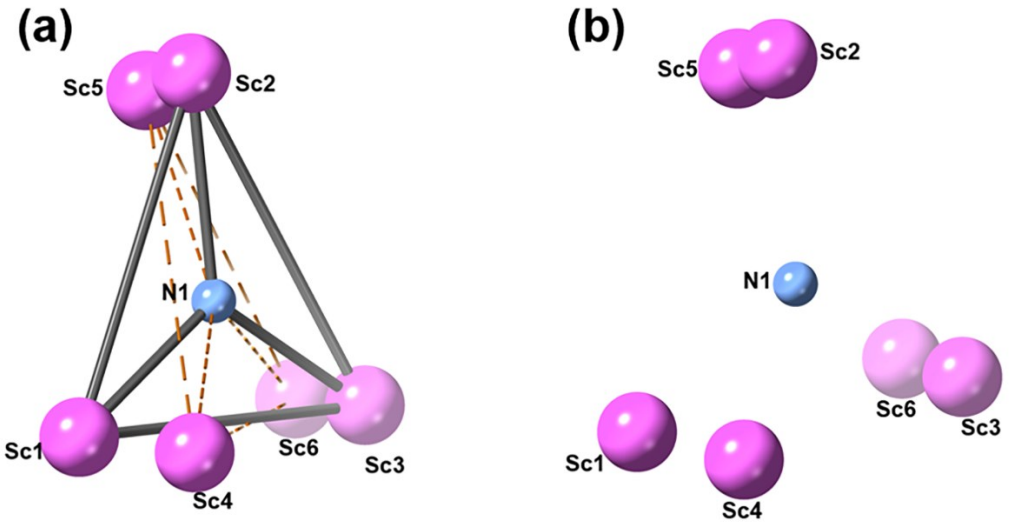

Fig. S3 (a) a diagram showing the relative orientation of the two different triangular Sc_3N units. (b) Perspective drawing shows the disorder of Sc in the Sc_3N cluster. N atom is fully ordered.

Table S1. Comparison of the distances between the metal and closest cage carbon for $Sc_3N@C_s(39663)$-C_{82} and $Gd_3N@C_s(39663)$-C_{82}[3] (distances are given in angstrom)

compound	M-C	Distance / Å
$Sc_3N@C_s(39663)$-C_{82}	Sc1-C1	2.329(6)
	Sc1-C5	2.316(6)
	Sc2-C49	2.272(6)
	Sc2-C50	2.280(6)
	Sc3-C59	2.340(5)
	Sc3-C60	2.256(5)
$Gd_3N@C_s(39663)$-C_{82}	Gd1-C78	2.476(10)
	Gd1-C82	2.48(10)
	Gd2-C28	2.370(8)
	Gd3-C17	2.438(9)
	Gd3-C18	2.429(8)

Table S2. Occupancy of disordered Sc site in the Sc_3N cluster.

Atom	Sc1	Sc2	Sc3	Sc4	Sc5	Sc6
Occupancy	0.817	0.817	0.817	0.183	0.183	0.183

Table S3. Bond lengths and bond angles of the Sc_3N cluster in the major orientation.

	Sc1-N1	Sc2-N1	Sc3-N1
Length (Å)	2.112(3)	2.052(4)	2.038(3)
	Sc1-N-Sc2	Sc1-N-Sc3	Sc2-N-Sc3
Angle (°)	118.05(17)	117.45(14)	124.43(18)

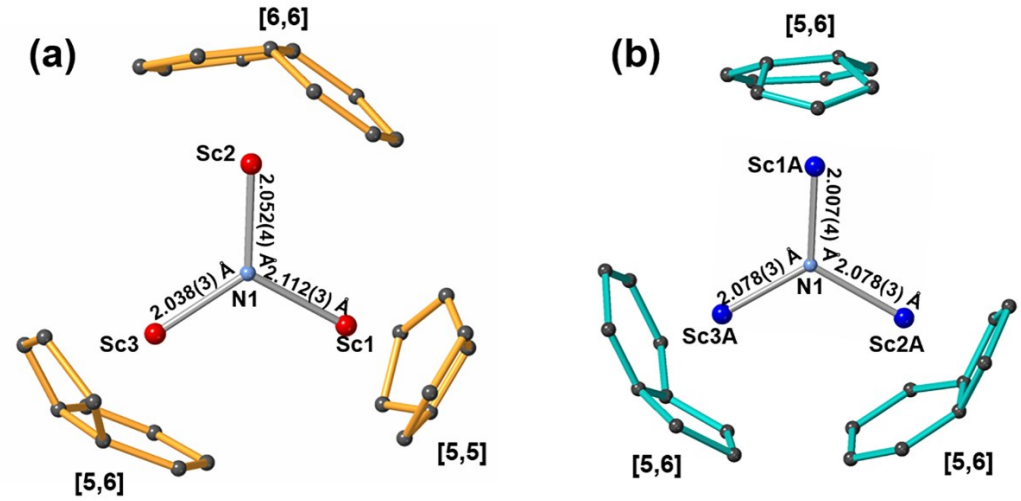

Fig. S4 Comparison of the endohedral structures of $Sc_3N@C_s(39663)$-C_{82} (a) and $Sc_3N@C_{2v}(39718)$-C_{82} (b).

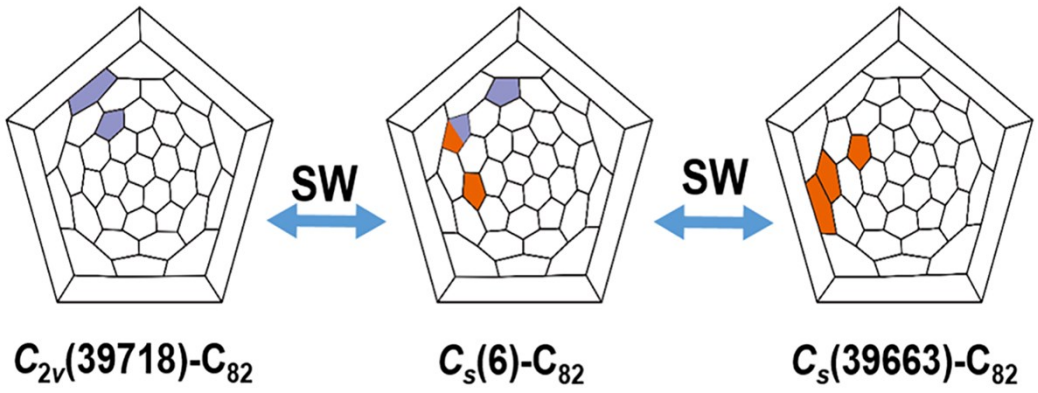

Fig. S5 Stone-Wales transformation of $C_s(39663)$-C_{82}, $C_s(6)$-C_{82} and $C_{2v}(39718)$-C_{82}.

Reference

1 Dolomanov, O. V.; Bourhis, L. J.; Gildea, R. J.; Howard, J. A. K.; Puschmann, H., *J. Appl. Crystallogr.,* 2009, **42**, 339-341.

2 Sheldrick, G., Acta Crystallogr., Sect. C: Struct. Chem., 2015**, 71**, 3-8.

3 Mercado, B. Q.; Beavers, C. M.; Olmstead, M. M.; Chaur, M. N.; Walker, K.; Holloway, B. C.; Echegoyen, L.; Balch, A. L., *J. Am. Chem. Soc.,* 2008**, 130**, 7854-7855.